Natural Resources for Human Health

eISSN: 2583-1194

Original Research

Received 16 May 2026
Revised 16 June 2026
Accepted 04 July 2026

Natural Resources for Human Health 2026, Vol. 6 (4s): 819–831

KEYWORDS:
Seam carving, saliency detection, reflection, energy map, image resizing, Morphological Image Processing

Content-Aware Image Retargeting with Reflection-Aware Energy Augmentation and Boundary-Preserving Seam Optimization

Arjun Rai Dutta[1], Surbhi Saroha[2], Ankit Garg[3]

[1]School of CSE, Shobhit University, Meerut, India
[2] School of CSE, Shobhit University, Meerut, India
[3] UCRD, UIE, Chandigarh University, Mohali, Punjab, India
*Corresponding author: ankitgitm@gmail.com

ABSTRACT: Seam carving (SC) deforms reflective regions and object boundaries by eliminating lowcost seams. To address this limitations, this paper integrates proposed augmented map (PAM) with proposed image morphology-based retargeting algorithm (PIMRA). The PAM is the fusion of multiple operators such as the base energy map, reflection likelihood map, and saliency map. The PIMRA comprises dilation and erosion operations for energy augmentation along objects boundaries and reflective areas. The integration of PAM and PIMRA is assessed against existing state of arts such as scaling, cropping, SC, and Multi-Operator. The comparative analysis is performed based on parameters such as brightness, contrast, structure, distortion on edges and gradients, noise, and reflectance alignment. The user study presents the efficacy of PIMRA in preserving structure, naturalness, reflection realism, and adaptability. Results confirm that the PIMRA integrated with PAM effectively preserves reflective regions and maintains object boundary integrity during image resizing.

1. INTRODUCTION

Nowadays, manufacturers of mobile phones, televisions, smartwatches, etc., are producing multimedia devices with varying screen sizes. Therefore, images must be resized according to the device screen's aspect ratio. Researchers have proposed so many methods to alter the size of an image. Conventional methods, such as cropping, warping, and SC, produce loss of information while the resizing operation is performed on the images. The main objective of all the proposed retargeting methods should be the preservation of information loss and the structure preservation of objects present in the image. Avidan et al. [1] proposed a Content-aware image retargeting (CAR) i.e., SC, to resize the image in a content-aware fashion. Although the SC technique preserves the visually appealing regions, it has some limitations [2]. SC utilizes a conventional gradient-based energy map, which misclassifies prominent reflective regions, leading optimal seams to be passed over them. As a result, pixels are eliminated from the reflective regions, which produce a visual artifact in the image [3-4]. Another challenge of SC is to segregate the foreground and background regions when the color of their boundaries is almost the same. In this case, the optimal seams cover both regions and distort the structure of salient objects present in the image. This work mainly focuses on the problem of preserving reflection continuity and object boundary integrity during CAR. To get rid of these challenges, an efficient augmented map is proposed, which trace reflective regions as an important part of the image. The integration of PAM with the PIMRA increases the reflective-awareness and ensure that optimal seams do not pass over the reflective regions. In addition to this, conventional SC is improved using energy augmentation and morphological operations so that the structure of foreground and background regions can be preserved even if their boundary color is almost the same. The main objectives of the proposed work are listed below.

(a) Reflection Preservation: Prevent seam removal from reflection-sensitive regions using a PAM. The PAM effectively identifies the reflective regions and other important objects.

(b) Integration: Integration of PAM with PIMRA to preserve objects present in the image.

(c) Object Boundary Protection: To introduce image morphological operation in PIMRA to mitigate deformation on foreground and background objects when their color composition is same.

(d) Performance Evaluation: To assess the performance of PAM and PIMRA using quantitative metrics.

(e) Comparative analysis: To conduct a comparative analysis among proposed work and existing state of arts.

Preserving reflective regions is a significant challenge in digital imaging. Reflections often carry semantic meaning—like buildings reflected in glass, cars reflected in glossy paint, or natural objects mirrored on water surfaces. Distortion of such reflections results in visually unrealistic retargeted images. Improving SC for reflection preservation can enhance CAR for photography, digital media publishing, surveillance imaging, advertising display performance, and AR/VR visualization. This motivated the development of a PAM and PIMRA that can intelligently protect reflection continuity and object boundaries while resizing images. The scope of this research is limited to 2D static image retargeting. The integration of PAM and PIMRA only focuses on preserving reflective regions and is applicable to images with glossy surfaces, mirrors, lakes, or metallic objects. Integration of PAM and PIMRA does not currently address video retargeting, computational efficiency enhancement, or deep learning-based acceleration. These can be explored as future extensions.

2. LITERATURE REVIEW

2.1. Shadow and Reflection Preservation Techniques

Hashemzadeh et al. [5] proposed a shadow-sensitive SC to detect the regions having shadow objects. The novelty of proposed technique is to model shadow regions as sensitive areas to avoid seam intrusion. Patel et al. [6] introduced a novel retargeting algorithm that preserves reflection symmetry during resizing. The novelty of the proposed technique is to introduce reflection-symmetry detection and utilizing symmetry constraints to guide seam selection. Garg et al. [7] proposed a shadow preservation framework for CAR by constructing an efficient importance map. The novelty lies in integrating shadow information with the seam diversion-based image retargeting (SDIR) process to reduce distortions.

2.2. Multi-Op based Image Retargeting Technique

Abhayadev et al. [8] proposed a technique that combines saliency-based scaling with SC adaptively. Garg et al. [3] proposed an improved Multi-Op scheme to mitigate structural deformations on the prominent objects. Zhou et al. [9] proposed a technique that uses weak supervision and reinforcement strategies to select operators per region. Fragoso-Navarro et al. [10] proposed technique embeds watermarks robust to seam-carving; modifies seam costs to protect watermark regions. Guo et al. [11] proposed a Multi-Op based retargeting pipeline that fuses SC, scaling, and other retargeting operators based on saliency ranking and similarity assessment. Garg et al. [12] proposed a hybrid sequence of retargeting operators to preserve structure of image objects during resizing. Sun et al. [13] proposed deep multi-target image retargeting (MulTIR), capable of retargeting towards multiple target sizes and aspect ratios within a single model.

2.3. Learning-Based and Deep Neural Network Approaches

Mei et al. [14] proposed a supervised deep network for image retargeting trained on a retargeting dataset. Guo et al. [15] proposed a learning-based image retargeting network that uses relative saliency maps to guide retargeting. Xu et al. [16] introduced human-aligned end-to-end image retargeting with layered transformations, which decomposes images into salient and non-salient layers, applying different transformations and a perceptual structure-similarity loss.

2.4. Energy Optimization and Seam Diversion Methods

The previous approaches emphasized operator or learning integration, this category focuses on fundamental energy formulations and seam optimization mechanisms. Garg et al. [17] proposed a modified SC method that integrates image stitching to merge disjoint image segments and prevent artificial seams during resizing. Garg et al. [18] proposed an efficient energy function to increase energy of pixels where optimal seam intersect each other. The objective is divert optimal seams to nearby regions to suppress distortion over straight lines. Garg et al. [19] performed a performance analysis of a SDIR technique to calculate its time complexity.

2.5. Saliency- and Attention-Guided Image Retargeting

Ahmadi et al. [20] proposed a CNN-based method that enhances image retargeting by incorporating context-aware saliency detection. Li et al. [21] proposed a plug-and-play framework to adapt static image saliency models for dynamic video data. Jiang et al. [22] proposed a technique that u*ses* saliency guidance for image translation tasks—techniques transferable to retargeting pipelines. Aberman et al. [23] proposed a saliency-guided image optimization technique that adjusts visual elements to minimize distraction and enhance attention focus. Imani et al. [24] proposed a deep learning–based stereo video retargeting framework that detects and preserves salient objects during resizing. Zhang et al. [25] proposed a technique that integrates gaze distributions and saliency models for content-preserving editing.

2.5. Analysis and Survey Work

Zhang et al. [26] proposed a focused analysis and evaluation framework for measuring quality of content-aware retargeted images. Garg et al. [27] presented a survey on CAR techniques. The novelty lies in the comparative analysis of major resizing methods. Wei et al. [28] proposed a reduced-reference IQA method tailored for retargeted images. The novelty shows the uses of local and global features and Earth Mover's Distance to measure how well reference content is preserved after retargeting. Tang et al. [29] proposed a saliency-driven quality assessment for retargeted images. Garg et al. [30] proposed an improved SC technique that utilizes a gradient-based energy map to preserve important image content during resizing. Additionally, the limitations and possible solutions are suggested to reduce distortions during retargeting. Fan et al. [31] proposed work summarizes advances, datasets, metrics and challenges in the field of image retargeting.

3. PROPOSED METHODOLOGY

PIMRA efficiently separates foreground and background regions with low color contrast by strengthening weak edges through energy augmentation and morphological operations, which divert seams toward less important areas and prevent deformation of key objects. When combined with PAM, it further protects object boundaries and reflective semantic regions. Overall, the framework achieves two main goals: (i) preserving structural integrity and (ii) protecting reflection-sensitive regions during image retargeting. The method operates in two phases: Phase- 1 builds PAM to highlight reflective areas, and Phase-2 performs morphology-guided seam optimization and integrates PAM with PIMRA for refined seam selection and diversion.

3.1. Phase-1 (Generation of PAM)

The phase-1 focuses on constructing a perceptually enriched augmented map that highlights visually important reflective regions. The steps needed to develop PAM are given below.

Step 1: In this step a gradient symmetry analysis is performed to identify the symmetrical patterns which are the reflective surfaces present in the image.

In step 1, a symmetry score $S(x, y)$ is computed to obtain the bilateral similarity around each pixel using Eq. (1).

$$G(x_i, y_i) = \sum_{(i,j)\in W} |K(x+i, y+j) - K(x-i, y-j)| \quad (1)$$

where W represents the size of local window placed at (x_i, y_i), $K(x, y)$ showcases the image intensity at pixel (x, y), $G(x_i, y_i)$ presents higher bilateral similarity.

Step 2: In this step intensity & contrast detection is performed to highlight the difference between luminance (brightness) and contrast based on the obtained values. In step 2, intensity normalization is performed using histogram equalization. Let $I(x, y)$ denote the original grayscale image. To standardize intensity distribution and enhance contrast, a histogram equalization is applied using Eq. (2).

$$I\_h(x, y) = H\_e(I(x, y)) \quad (2)$$

where $I\_h(x, y)$ is the normalized intensity image and $H\_e(\cdot)$ denotes the histogram equalization operation.

Further, in step 2, luminance thresholding is performed to detect regions exhibiting high brightness. To compute a dynamic luminance threshold Eq. (3) and (4) are used.

$$L\_T = \mu + \alpha \cdot \sigma \quad (3)$$

eISSN: 2583-1194

$$R_{L(x,y)} = \begin{cases} 1 \; if(I\_h(x,y) > L\_T \\ 0 \quad\quad Othersie \end{cases} \tag{4}$$

In Eq. (3) μ and σ showcase the mean and standard deviation of $I\_h\ (x,y)$ and α represents a tunable scalar parameter in range (1.0-2.0).

Further, local contrast is computed within a neighborhood window W(5×5 pixels) centered at each pixel. The details of the methods used for this purpose are given below.

(a) Max–Min Contrast: Max-min contrast calculates the difference between the brightest and darkest pixels in a local window W centered at (x,y) using Eq. (5).

$$CO_{max-min}(x,y) = \max_{(i,j)\,\in\, W} I\_h(i,j) - \min_{(i,j)\,\in\, W} I\_h(i,j) \tag{5}$$

where $CO_{max-min}(x,y)$ represents max-min contrast at a pixel position (x,y), $I\_h(i,j)$ represents normalized intensity value, W depicts local window, $\max_{(i,j)\,\in\, W} I\_h(i,j)$ depicts the maximum intensity value within the window, and $\min_{(i,j)\,\in\, W} I\_h(i,j)$ showcases the minimum intensity value within the same window.

(b) Local Standard Deviation: Local standard deviation measures the variation of intensity value

from the local mean within a window W, as defined in Eq. (6).

$$C_{stand}(x,y) = \sqrt{\frac{1}{|W|}\sum_{(i,j)\in W}(I\_h(i,j) - \overline{IW})^2} \tag{6}$$

where $\overline{IW}$ represents the average intensity in window W and $|W|$ showcases the number of pixels inside W.

The contrast threshold T_C is applied to generate a binary contrast map using Eq. (7).

$$R_C(x,y) = \begin{cases} 1 \; if C(x,y) > T_C \\ 0 \quad\quad Othersie \end{cases} \tag{7}$$

Finally, the final reflection likelihood map $RI(x,y)$ is computed by combining the luminance and contrast maps using Eq. (8).

$$RI(x,y) = R_L(x,y).R_C\ (x,y) \tag{8}$$

This map identifies likely reflection pixels $(RI(x,y) = 1)$ and non-reflection regions $(RI(x,y) = 0)$.

Step 3: This step is used to identify the reflective regions using deep learning. Deep saliency-guided filtering uses pre-trained convolutional networks like U^{2}Net, R3Net, or BASNet that learn multi-level contextual and semantic attention from large-scale datasets, in contrast to traditional saliency methods that only use color or contrast cues. The pixel-wise saliency probability map $S(x,y)$ generated by the deep saliency model in the suggested framework draws attention to visually noticeable areas like glossy borders, metallic textures, and reflective surfaces. The reflection likelihood map obtained from Step-2 is used as a guidance mask in a guided filtering operation to prevent confusion between reflective highlights and non-reflective bright areas (such as the sky or illumination). Salient reflective regions are emphasized while irrelevant bright zones are suppressed in the filtered saliency map $S_f(x,y)$.

Given an input image $I(x,y)$, the saliency network outputs a saliency map which is given in Eq. (9)

$$DS(x,y) = SaliencyNet(I(x,y)) \tag{9}$$

where $DS(x,y) \in [0,1]$ indicates the probability of each pixel belonging to a visually salient region.

The accuracy of reflection preservation during SC is increased by creating a strong reflection-aware mask by fusing this filtered saliency data with the reflection likelihood map in Step 4.

Step 4: Fuse Reflection Likelihood Map & Saliency Map- This step is used to identify the significant areas that contain reflective areas in the image. After fusion of both the maps obtained from Step 2 & 3, a final reflection-aware mask is generated. By ensuring that only salient regions that are consistent with reflection cues are included in the final reflection mask. The deep saliency-guided filtering helps to improve semantic consistency and decrease false positives.

In step 4, the final reflection mask $M_{reflect}(x, y)$ is computed by fusing the complementary information obtained from gradient symmetry analysis, intensity-contrast reflection likelihood, and optionally deep saliency-guided filtering. This weighted fusion enhances the accuracy and robustness of reflection region detection.

Formally, the mask is obtained using Eq. (10)

$$M_{reflect}(x, y) = \omega_1.\left(1 - \hat{S}(x, y)\right) + \omega_2.RI(x, y) + \omega_3.\widehat{DS}(x, y) \qquad (10)$$

where $\hat{S}(x, y)$ is the normalized gradient symmetry score map, $RI(x, y)$ is the binary reflection likelihood map, and $\widehat{DS}(x, y)$ is the normalized deep saliency map. $\omega_1, \omega_2, \omega_3$ are tunable weights controlling the contribution of each component.

After fusion, the continuous mask $M_{reflect}$ is binarized using Otsu's thresholding or an adaptive thresholding method to precisely segment reflection zones.

Step 5: Augmented Energy Map Creation- The base energy map obtained after applying morphological operation is further fused with the final reflection-aware mask to obtain the PAM. The PAM guides the PIMRA to eliminate those regions of the image that are not important. In step 5, to effectively preserve reflection regions during SC, the final reflection mask $M_{reflect}(x, y)$ is utilized to augment the conventional energy map. Typically, the base energy map $E_{base}(x, y)$ is computed using image gradient operators (e.g., Sobel) to highlight salient edges and structures in the image. The obtained based energy map then fused with final reflection mask $M_{reflect}(x, y)$ to create an augmented map. The reflection mask, which indicates the spatial locations of reflection regions, is incorporated by adding an energy penalty term weighted by a factor λ. The PAM $E_{Aug}(x, y)$ is formulated in Eq. (11).

$$E_{Aug}(x, y) = E_{base}(x, y) + \lambda \cdot M_{reflect}(x, y) \qquad (11)$$

where $\lambda > 0$ controls the degree to which reflection areas are protected.

Higher energy penalties are assigned to seams traversing these reflection regions, discouraging seam removal or distortion within reflections and thus preserving their visual integrity during CAIR or manipulation. Since $M_{reflect}(x, y)$ typically assumes binary or probabilistic values emphasizing reflection zones, this addition increases the energy values in those areas. Consequently, the SC algorithm is discouraged from selecting seams that pass through reflection regions, thereby reducing distortions and preserving important reflection details. The proposed methodology employs the final reflection mask $Mreflect(x, y)$ as a core component during the retargeting process. For each image category, the mask identifies the most perceptually significant reflection regions—whether specular or diffuse—by leveraging the fusion of gradient symmetry, reflection likelihood map, optional deep saliency-based filtering, and base energy map. This mechanism preserves essential visual details and prevents perceptual artifacts during resizing operations.

Step 6: Integration of PAM with PIMRA: In this step, the PAM obtained from Step- 5 is integrated with PIMRA. The PAM assigns higher energy values to ROIs where reflective areas are present. In this manner, the prominent reflective surfaces can be preserved while optimal seams try to select the least energy value pixels. The flow of phase-1 is shown in Fig. 1.

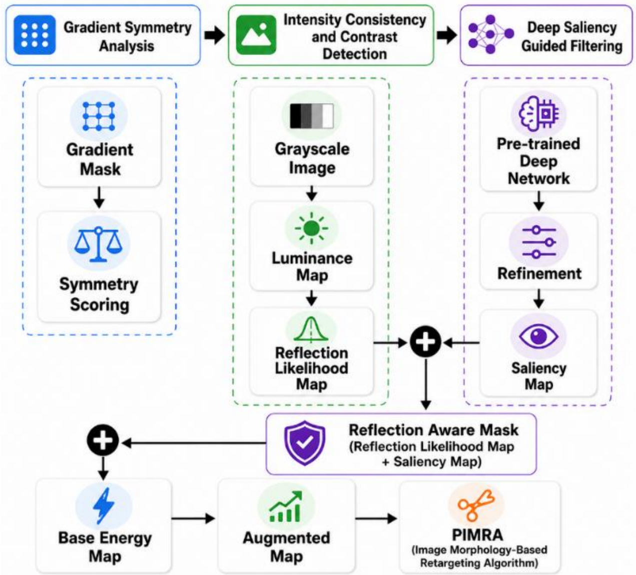

Figure 1. Proposed methodology: flow of phase-1

3.2. Phase -2 (Morphology-Guided seam optimization)

SC produces deformations while image contains low contrast boundaries between foreground and background regions and due to similar color compositions among them. The SC is improved using morphology-guided seam optimization. In the PIMRA morphological operations are performed to increase the width of object boundaries.

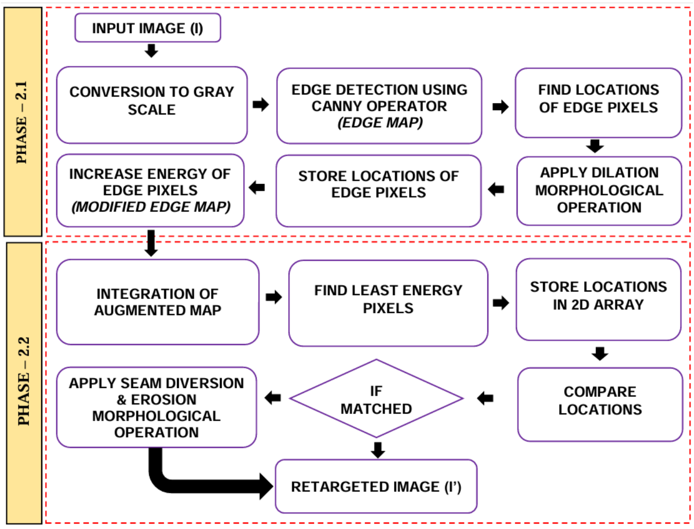

Figure 2. Proposed Methodology: Flow of Phase-2

After this, an energy augmentation operation is performed to increase the energy of pixels present on object boundaries. When both operations are applied in combination, the optimal seams are diverted before reaching the object boundaries. As a result, distortion of the objects is effectively suppressed. The entire flow of PIMRA is shown in Fig. 2.

3.2.1. Morphology and Energy Augmentation

In this phase, prominent edges are first detected using the Canny operator. Morphological dilation (and erosion, using disk-shaped structuring elements) is then applied to widen object boundaries and form protective zones. The energy of boundary pixels is increased to create a base energy map, which discourages seams from crossing object edges. This base map is combined

eISSN: 2583-1194

with the reflection-aware mask to form the augmented map, guiding seams away from important regions and reducing structural loss in ROIs during retargeting.

3.3. Dataset Selection and Categorization

To assess the performance of proposed framework some images are selected from SIR² dataset. The dataset contains images in which reflection regions are present with diverse lighting conditions. The dataset is mainly selected to showcase the presence of different reflection strengths inside the images taken for analysis and experiments. The dataset also provide the information about the ground-truth background and different reflection components present in the image.

3.4. Assessment Types and Methods

To assess the performance of the PIMRA objective and subjective assessments are conducted. A total of five methods such as SSIM, PSNR, GEL, and SPI are selected to perform objective analysis on the results obtained from cropping, scaling, SC, Multi-Op. To efficacy of the PIMRA is justified based on some parameters such as Luminance, Contrast, Structure, Pixel-wise MSE, Gradient magnitude, and Structure preservation [31]. The chosen methods are selected as they collectively measure four different aspects such as overall structure of the image objects, pixel-level accuracy, edges and boundaries preservation, and visual similarity. These all aspects are important in CAR which judging the efficiency of proposed algorithm. To perform subjective analysis a total of six observers are chosen based on their experience in the field of image processing. The observers provide ratings on the retargeted outcomes produces by different methods. In the subjective analysis five parameters are chosen such as content preservation, reflection realism, visual naturalness, efficiency, and adaptability.

4. DEVELOPMENT OF PIMRA

PIMRA tries to overcome the limitation of SC specifically for the scenes in which foreground and background regions are separated by either low contrast boundaries or having the same color. The PIMRA strengthens such type of boundaries using an energy augmentation operation. To divert the optimal seams before entering inside the salient objects, image morphological operations are carried out. The inclusion of image morphological and energy augmentation operations, the diversion of the optimal seams to the nearby areas maintain the structural properties of the objects. Integration of PAM with PIMRA provide more strength to PIMRA to detect and preserve reflective-regions and maintain clear foreground–background separation in the entire retargeting operation.

4.1. PIMRA: Phase 2.1 (Base Energy Map Generation)

In phase 2.1 mentioned in Fig. 2, the primary objective of PIMRA is to separate foreground and background regions by applying image morphological operation. Firstly, a canny operator is applied to detect prominent and weak edges present in the images. Secondly, Gaussian smoothing and pixel connectivity analysis is performed to reduce noise and to obtain the perimeter pixels, respectively. Thirdly, the identified prominent and weak edges are binarized using Otsu's thresholding [32]. The main objective of the third step is to clearly separate foreground and background regions. Fourthly, on identified edges, a dilation operation is performed to increase the width of the edges. Finally, through an energy augmentation operation, the energy of the edge pixels is increased to develop a shielding zone around the object boundaries. After applying morphology and energy augmentation a modified energy map called base energy map is generated. To obtain a more accurate augmented map, both the base energy map and PAM is combined, shown in phase-2.2.

4.2. PIMRA: Phase-2.2

In Phase 2.2, the PAM is combined with the base energy map to develop augmented map. The main objective of integration is to preserve prominent reflective regions and foreground–background regions. The PIMRA perfectly utilizes the augmented map to find out the path of least energy pixels from the image using dynamic programming. PIMRA integrated with the augmented map astutely take care about the reflective regions, object boundaries and visual naturalness of the retargeted outcome. After elimination of seams an erosion operation is applied is applied invert the impact of dilation operation over the object boundaries. The seam diversion operations is applied before the dilated boundaries of object so that optimal seams do not cross the salient object. Therefore, the weak boundaries remains unaffected.

5. RESULTS AND DISCUSSION

In this section results obtained from different proposed pipelines are presented. Fig. 3 showcases the results obtained from the pipeline of PAM generation.

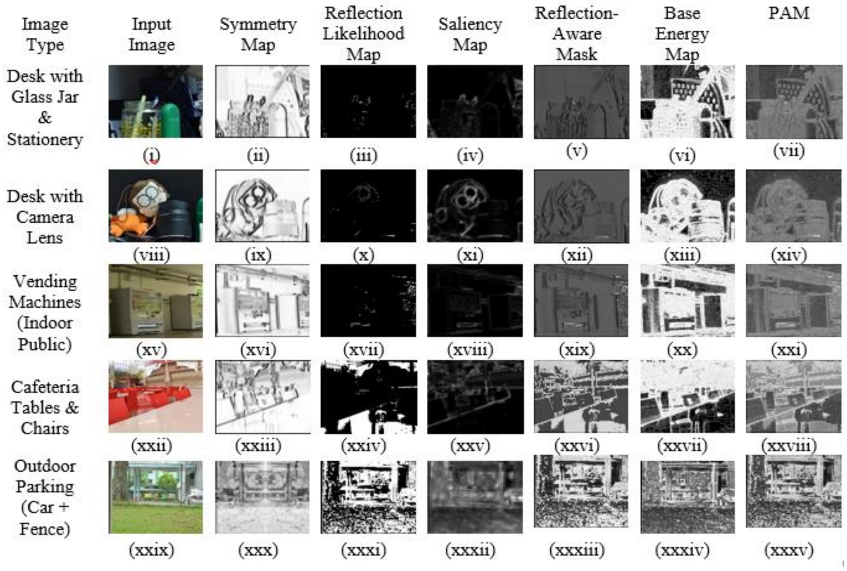

Figure 3. Pipeline to generate PAM on SIR² dataset images

To obtain the results, five images (two indoor and three outdoor) are selected from the SIR² dataset, in which a rich set of reflective regions is presented. From the chosen images, a set of results are generated which shows symmetry map, reflection likelihood maps, deep saliency maps, and reflection-aware mask. The second last column shows the results obtained after applying the morphological and energy augmentation operation over the detected objects boundaries. The last column shows the results obtained after integrating the reflective-aware mask and the base energy map. From the PAM is can be visualize that reflective regions are clearly highlighted and the width of objects boundaries is increased with high energy value. The non-reflective regions and least important regions are unchanged.

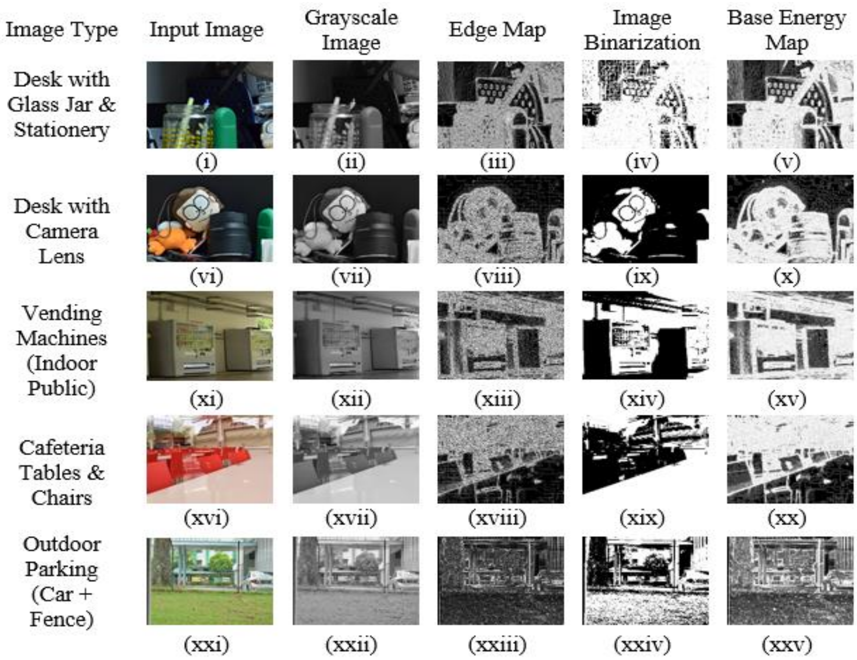

Figure 4. Pipeline to generate base energy map on SIR² dataset images

eISSN: 2583-1194

Fig. 4 showcases the results obtained from the pipeline of the base energy map. The edge maps presented in the third column show the prominent edges present in the image, which need to be preserved during the retargeting operation. In the third column, the prominent and weak edges are binarized using Otsu's thresholding to clearly separate foreground and background regions. Finally, in the last column, base energy maps are presented, which are developed after applying morphological and energy augmentation operations. Fig. 4 presents the effectiveness of the base energy map after applying edge detection and image binarization operations. The low contrast boundaries and separation of foreground and background regions can be clearly visualized in the results present in the last column. The effectiveness of the dilation operation can be visualized in the base energy maps, which are used to widen object boundaries.

Fig. 5 presents the complete pipeline of PIMRA on the chosen image from the SIR² dataset. In this figure, the first column presents different categories of images, the second column shows the original input images, and the third column presents the results of the augmented map, which is the integration of the reflection-aware mask and base energy map.

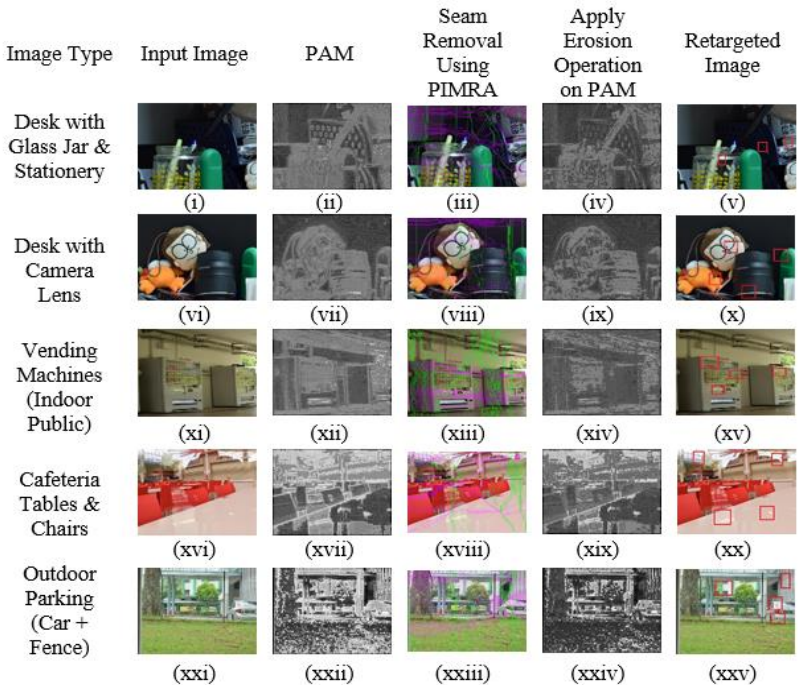

Figure 5. Pipeline to generate retargeted results on SIR² dataset images

From the results shown in column two, it can be observed that PAM is capable of widening the prominent edges, highlighting reflective regions, and clearly separating foreground and background regions. Results depicted in the fourth column show the generation of an optimal seam after integration of PAM with PIMRA. Multiple optimal seams are generated in different areas of the image. In the process of PIMRA, multiple seam diversion operations are carried out due to the execution of image morphological and energy augmentation operations. The areas in which high energy is present are protected from any kind of distortion, such as reflection discontinuity and other artifacts. In the fifth column, the effect of the erosion operation can be observed, which reduces the effect of the dilation operation on the prominent edges of objects. Finally, the sixth column represents the retargeted results obtained from PIMRA. In the results, it can observe that reflective-regions such as glass, lenses, vending machines, the reflection of a white table, and car glass are protected. In all these images, multiple regions are available in which color of foreground and background is almost same. Due to which foreground and background objects are separated by weak object boundaries. This problem is also resolved by PIMRA by applying energy augmentation and morphological operations.

6. COMPARISON AND VISUAL IQA

This section compares the retargeting outcomes obtained from PIMRA and other state-of-the-arts. The comparision of PIMRA and stae-of-the-arts is shown in Fig. 6. The images are selected from the SIR² dataset, in which challenging attributes of reflective regions and weak separation of foreground and background objects are present. The conventional scaling method distort salient object when the aspect ratio of the image alters both in horizontal and vertical directions. Uniform scaling produces visual atrifacts on different attributes of objects such as lines, circle, reflections, background, and foreground. Cropping techniques eliminate important regions of dominating objects as the surrounding cut increases the loss of context of the scene. SC do not consider reflective regions, shadow regions as important objects, and eliminates pixels using dynamic programming. The main cause of distortion is due to the use of a conventional gradient based energy map. Multi-Op methods improve the results of retargeting by combining multiple retargeting operators.

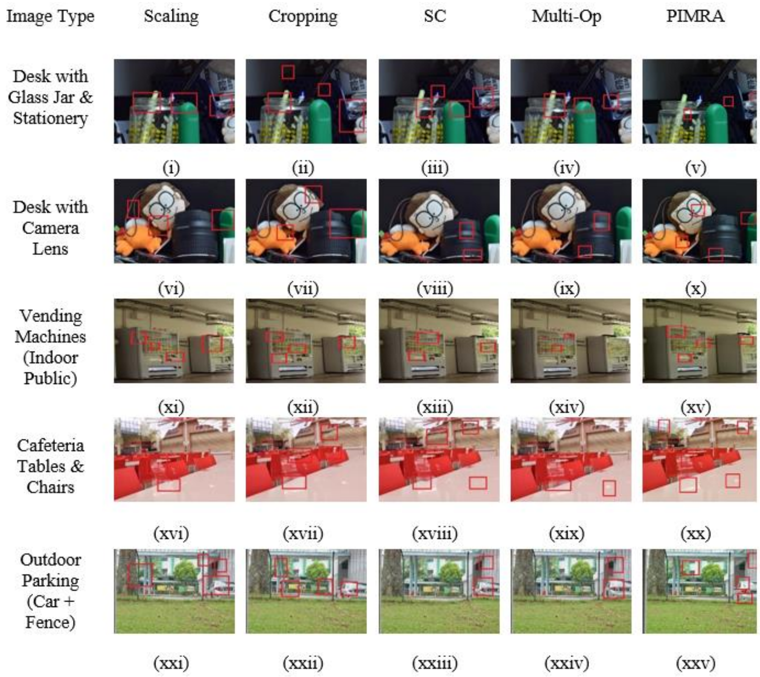

Figure 6. Retargeted results obtained from state-of-the-arts and PIMRA

The time taken by the Multi-Op technique is significantly high as compared to single operator. The results shown in the figure presents less deformations of objects present in the image. The results obtained from PIMRA generate better retargeting outcomes as compared to existing state of the arts. In the results of PIMRA reflection on the table, the jar, the glass of the car, and the glass of the vending machine are highly preserved from distortion. The obtained results from all the techniques cannot be compared directly by the human visual system. Therefore, all the outcomes require quantitative and subjective analysis using comparison metrics and experts respectively. In section 6.1, objective analysis is performed using SSIM, PSNR, GEL, and SPI. The details of the subjective analysis are given in section 6.2.

6.1. Objective IQA

Fig. 7 compares all the chosen categories of images using SSIM, PSNR, GEL, and SPI. The comparative analysis is performed using state-of-the-art techniques such as scaling, cropping, SC, and Multi-Op. From the objective analysis, it is observed that PIMRA performs well for all the chosen categories of images. The details of the objective IQA are given below.

- SSIM (↑ better): PIMRA achieves the highest structural similarity, showing about 8% improvement over Cropping and ~0.6% over Multi-Op, meaning better perceptual quality and structure preservation.
- PSNR (↑ better): PIMRA records the highest PSNR, giving around 21% improvement over Cropping and ~2.4% over Multi-Op, indicating lower pixel-level distortion.
- GEL (↓ better): PIMRA has the lowest gradient error loss, showing nearly 51% reduction compared to Cropping and about 7.8% improvement over Multi-Op, which means edges and gradients are better preserved.

- SPI (↑ better): PIMRA achieves the highest structure preservation, with about 12.6% improvement over Cropping and ~0.9% over Multi-Op, confirming stronger boundary and object integrity.

Overall, the figure clearly shows a performance trend from basic methods (Cropping, Scaling) → SC → Multi-Op → PIMRA, proving that PIMRA provides the best balance of perceptual quality, low distortion, edge preservation, and structural integrity.

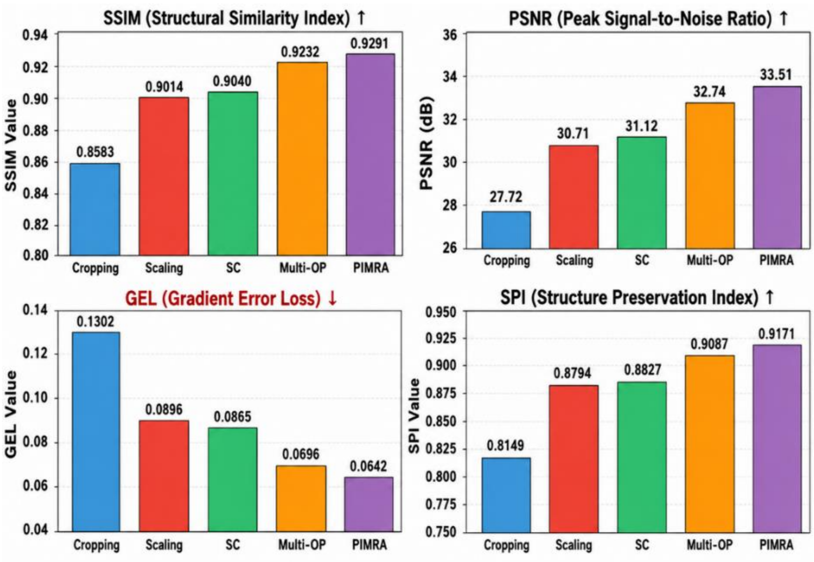

Figure 7. Comparison of Retargeting Outcomes Based on State-of-the-Arts and PIMRA

6.2. Subjective User Study

Fig. 8 shows a subjective evaluation (MOS scores from 6 experts) comparing Cropping, Scaling, SC, Multi-Op, and PIMRA across five perceptual parameters: Content Preservation, Reflection Realism, Visual Naturalness, Efficiency, and Adaptability. PIMRA receives the highest ratings in four out of five categories—Content Preservation (4.85), Reflection Realism (4.88), Visual Naturalness (4.80), and Adaptability (4.70)—showing superior perceptual quality and reflection preservation. Multi-Op ranks second, SC shows moderate performance, while scaling and cropping score lowest due to distortions and content loss. Cropping performs best only in efficiency because of its simplicity, highlighting a quality–computation trade-off for PIMRA. Smaller error bars for PIMRA indicate strong agreement among observers. Overall, the subjective results align with objective metrics, confirming that PIMRA delivers the most visually natural and reflection-preserving retargeted images.

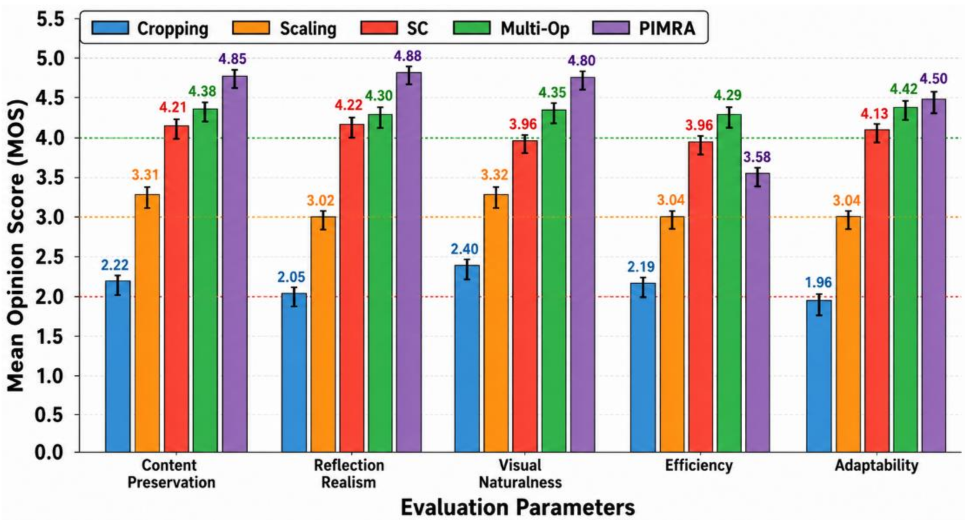

Figure 8. Subjective evaluation: grouped bar chart comparison (6 observers)

7. CONCLUSION AND FUTURE WORK

This paper addresses key limitations of SC in preserving reflective regions and object boundaries during content-aware resizing. SC often misclassifies smooth reflective surfaces as low-importance and fails in low-contrast foreground–background separation, causing artifacts and structural distortion. The proposed integration of PAM and PIMRA framework protects reflections using symmetry, reflection likelihood, and deep saliency cues, and preserves boundaries through morphology-based energy augmentation that diverts seams away from important structures. Experiments show consistent improvements over Scaling, Cropping, SC, and Multi-Op across SSIM, PSNR, GEL, and SPI, while a user study confirms better content preservation, reflection realism, visual naturalness, and adaptability. Overall, the framework effectively preserves reflections and object integrity. Future work includes deep learning–based end-to-end models, video retargeting with temporal consistency, GPU acceleration for real-time use, larger benchmark evaluations, reinforcement learning for operator selection, and unified multi-resolution retargeting models.

REFERENCES

[1] Avidan S, and Shamir A. (2007) Seam carving for content-aware image resizing. In Proc. of ACM SIGGRAPH 2007 papers, pp. 10-es. https://doi.org/10.1145/1275808.1276390

[2] Garg A, Singh A K. (2023) Analysis of seam carving technique: limitations, improvements and possible solutions. The Visual Computer, 39(7):2683-2709.

[3] Garg A, Negi A. (2020) Structure preservation in content-aware image retargeting using multi-operator. IET Image Processing, 14(13):2965-2975. https://doi.org/10.1049/iet-ipr.2019.1032

[4] Zhang Y, Sun Z, Jiang P, Huang Y, Peng J. (2017) Hybrid image retargeting using optimized seam carving and scaling. Multimedia Tools and Applications, 76(6):8067-8085. https://doi.org/10.1007/s11042-016-3318-1

[5] Hashemzadeh M, Asheghi B, and Farajzadeh N. (2019) Content-aware image resizing: An improved and shadow-preserving seam carving method. Signal Processing, 155:233-246. https://doi.org/10.1016/j.sigpro.2018.09.037

[6] Patel D, Nagar R, & Raman S. (2019) Reflection symmetry aware image retargeting. Pattern Recognition Letters, 125:179-186.

[7] Garg A, Ali A, & Kumar P. (2023) Original Research Article A shadow preservation framework for effective content-aware image retargeting process. Journal of Autonomous Intelligence, 6(3):245252.

[8] Abhayadev M, Santha T. (2019) Multi-Operator Content Aware Image Retargeting on Natural Images. Journal of scientific & Industrial Research, 78:193-198.

[9] Zhou Y, Chen Z, and Li W. (2020) Weakly supervised reinforced multi-operator image retargeting. IEEE Transactions on Circuits and Systems for Video Technology, 31(1):126-139. https://doi.org/10.1109/TCSVT.2020.2977943

[10] Fragoso-Navarro E, Rangel-Espinoza K, Nakano-Miyatake M. (2022) Seam Carving based visible watermarking robust to removal attacks. Journal of King Saud University-Computer and Information Sciences, 34(7):4499-4513.

[11] Guo Y, Wang D, Zhu Y, & Yan G. (2023) Multi-operator image retargeting based on saliency object ranking and similarity evaluation metric. Signal Processing: Image Communication, 119:117063.

[12] Garg A, Garg A, Singh A K, & Maram B. (2024) An Efficient Hybrid Sequence of Retargeting Operators to Minimize Structural Deformities in Image. In: International Conference on Nonlinear Dynamics and Applications, (pp. 509-523).

[13] Sun D, Guo Y, Yao C, Mei Y, Chen D, & Pan G. (2024) MulTIR: Deep Multi-Target Image Retargeting. In International Conference on Intelligent Computing, (pp. 124-133).

[14] Mei Y, Guo X, Sun D, Pan G, and Zhang J. (2021) Deep Supervised Image Retargeting. In 2021 IEEE International Conference on Multimedia and Expo (ICME), (pp. 1-6). https://doi.org/10.1109/ICME51207.2021.9428129

[15] Guo Y, Zhang M, Hao X, & Yan G. (2024) IRNet-RS: image retargeting network via relative saliency. Neural Computing and Applications, 36(8):4133-4149.

[16] Xu Y, Xie S, Li Z, Shadmany H. (2025) HALO: Human-Aligned End-to-end Image Retargeting with Layered Transformations, arXiv preprint arXiv:2504.03026.

[17] Garg A, Singh D, Saini M L. (2025) An Efficient Retargeting Technique to Mitigate Deformations by Integrating Seam Carving and Image Stitching. In 2025 2nd International Conference On Multidisciplinary Research and Innovations in Engineering (MRIE), (pp. 138-143).

[18] Garg A, Nayyar A, & Singh A K. (2022) Improved seam carving for structure preservation using efficient energy function. Multimedia Tools and Applications, 81(9):12883-12924.

[19] Garg A, & Singh A K. (2023) Performance analysis of seam diversion based image retargeting technique based on edge detection operators. Multimedia Tools and Applications, 82(15):23207-23250.

[20] Ahmadi M, Karimi N, & Samavi S. (2021) Context-aware saliency detection for image retargeting using convolutional neural networks. Multimedia Tools and Applications, 80(8):11917-11941.

[21] Li Y, Li S, Chen C, Hao A, & Qin H. (2020) A plug-and-play scheme to adapt image saliency deep model for video data. IEEE Transactions on Circuits and Systems for Video Technology, 31(6):2315-2327.

[22] Jiang L, Xu M, Wang X, & Sigal L. (2021) Saliency-guided image translation. In Proceedings of the IEEE/CVF Conference on Computer Vision and Pattern Recognition, (pp. 16509-16518).

[23] Aberman K, He J, Gandelsman Y, Mosseri I. (2022) Deep saliency prior for reducing visual distraction. In Proceedings of the IEEE/CVF Conference on Computer Vision and Pattern Recognition, (pp. 19851-19860.)

[24] Imani H, Islam M B, & Wong L K. (2023) Saliency-aware stereoscopic video retargeting. In Proceedings of the IEEE/cvf conference on computer vision and pattern recognition, (pp. 1230-1239.)

[25] Zhang Y, Wu N, Lin C Z, Wetzstein G, & Sun Q. (2024) Gazefusion: Saliency-guided image generation. ACM Transactions on Applied Perception, 21(4):1-19.

[26] Zhang T, Yu M, Guo Y, & Liu Y. (2019) Content-aware retargeted image quality assessment. Information, 10(3):111.

[27] Garg A, & Negi A. (2020) A Survey on Content Aware Image Resizing Methods. KSII Transactions on Internet & Information Systems, 14(7).

[28] Wei L, Zhao L, & Peng J. (2021) Reduced reference quality assessment for image retargeting by earth mover's distance. Applied Sciences, 11(20):9776.

[29] Tang Z, & Yao J. (2022) Image retargeting quality assessment based on saliency-driven classification. Signal Processing: Image Communication, 105:116688.

[30] Garg A, & Singh A K. (2023) Analysis of seam carving technique: limitations, improvements and possible solutions. The Visual Computer, 39(7):2683-2709.

[31] Fan X, Zhang Z, Sun L, Xiao B, & Durrani T S. (2024) A comprehensive review of image retargeting. Neurocomputing, 579:127416.

[32] Wu Q, Zhang G, Jing L, Yan J, & Liu Z. (2024) Binarization of road settlement monitoring point for autonomous rail rapid transit (ART) based on optimized Otsu algorithm. In Fourth International Conference on Computer Graphics, Image, and Virtualization, 13288:340-345.